PACS numbers: 42.55.Px; 42.60.Da; 42.60.Jf
DOI: 10.1070/QE2006v036n08ABEH013169

Spectral properties of a semiconductor α-DFB laser cavity

A.P. Bogatov, A.E. Drakin, D.V. Batrak, R. Güther, K. Paschke, H. Wenzel

***Abstract*. The experimental and theoretical investigations of spectral properties of a semiconductor α-DFB laser cavity are carried out. It is shown that in these lasers the curvature of mode gain spectra near the maximum is higher by more than two orders of magnitude than in conventional semiconductor lasers with a Fabry – Perot cavity. The distance between the adjacent axial modes of an α-DFB laser is shorter than in the case of a Fabry – Perot cavity laser of the same length, and its experimental value agrees well with the value obtained in the simple geometrical model, taking into account a zigzag propagation of radiation inside the cavity.**

Keywords: *heterolaser, α-DFB laser, cavity, spectral selectivity, Fox – Lee approach.*

1. Introduction

One of the promising types of a high-brightness semiconductor laser is the so called α-DFB laser that contains in its cavity a phase grating tilted by an angle α with respect to the cavity axis [1, 2]. The laser design and its operation scheme are given in Fig. 1. The phase grating is formed by producing the periodic spatial modulation of the effective (waveguiding) refractive index n in the cavity:

$$n(\boldsymbol{r}) = n_0 + \delta n \cos \boldsymbol{Q}\boldsymbol{r}, \tag{1}$$

where $\boldsymbol{r}$ is the radius vector of a point with coordinates y and z in the heterojunction plane; n_0 is the average effective refractive index; δn is the modulation amplitude; $\boldsymbol{Q}$ is the grating vector with components:

$$Q_y = \frac{2\pi}{\Lambda}\cos\alpha \text{ and } Q_z = -\frac{2\pi}{\Lambda}\sin\alpha; \tag{2}$$

where Λ is the grating period.

A.P. Bogatov, A.E. Drakin, D.V. Batrak P.N. Lebedev Physics Institute, Russian Academy of Sciences, Leninsky prosp. 53, 119991 Moscow, Russia; e-mail: bogatrov@sci.lebedev.ru;
R. Güther, K. Paschke, H. Wenzel Ferdinand-Braun Institute für Höchstfrequenztechnik, Gustav-Kirchhoff-Strasse, 4 D-12489 Berlin, Germany

Received 4 April 2006
Kvantovaya Elektronika **36** (8) 745 – 750 (2006)
Translated by D.V. Batrak

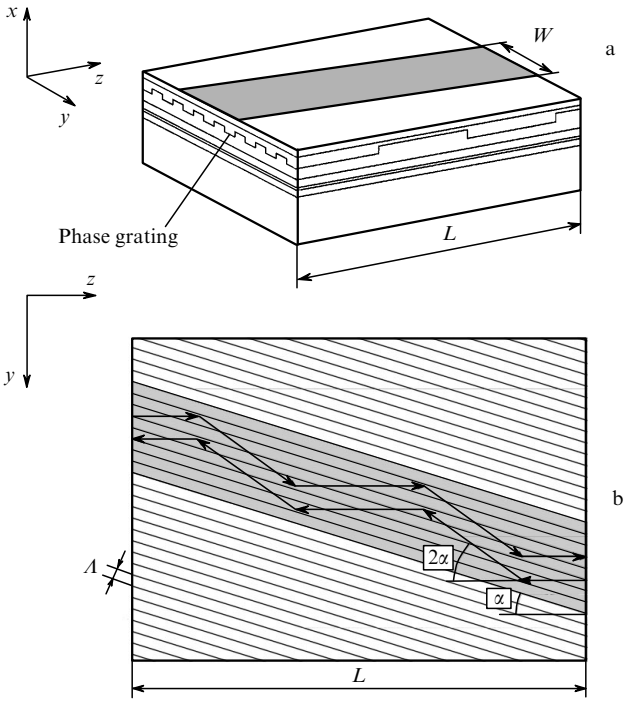

Figure 1. Scheme of the α-DFB laser design (a) and the principle of its operation (b). The pump region is shown in gray.

The vertical (along the x axis) field distribution is determined by the waveguide, which is formed by the heterostructure layers, and may be considered fixed, so that the direction along the x axis may be excluded from consideration, regarding propagation of light in this structure as two-dimensional. The refractive index of the medium in this case is assumed to take its effective value (the formal determination can be found, for example, in [3]). The variation of the effective refractive index is achieved by varying the thickness of one of the heterostructure layers.

If the emission wavelength in vacuum λ satisfies the Bragg condition

$$2\Lambda n_0 \sin\alpha = m\lambda, \quad m = 1, 2, \ldots, \tag{3}$$

where m is the diffraction order, then the main wave, i.e. the wave propagating along the laser axis (along z axis) will undergo diffraction, its energy being transferred to the energy of the diffracted wave. After passing some distance, virtually all of the initial energy of the main wave will

transform into the energy of the diffracted wave. Then this process will go in the reverse direction until the emission energy returns almost entirely to the main wave. Hence, the propagation of the emission in this structure takes a zigzag form. The average propagation direction for the wave satisfying the Bragg condition coincides with the direction of the grating lines, i.e., at an angle α to the laser axis, and the wave always remains in the pumped region, which is also tilted at the same angle α with respect to the cavity axis (Fig. 1b). Therefore, the phase grating operates as an effective spatial and spectral filter, providing a uniform transverse distribution of the field amplitude, corresponding to the zeroth transverse mode, and favours a single-longitudinal-mode operation.

Note that unlike the DFB laser, the presence of grating in an α-DFB laser does not lead to the appearance of a forbidden band in the spectrum. In the α-DFB laser, the propagation of a coupled wave pair is codirectional and periodical, whereas in the DFB laser the coupled waves propagate in the opposite directions and decay asymptotically, giving rise to a forbidden band in the transmission spectrum of the DFB structure.

The achievement of a 3-Watt cw output power in α-DFB lasers in the single-frequency regime with the optical beam divergence only 2–3 times larger than the diffraction limit was reported in [4, 5]. The spectral properties of the α-DFB-laser cavity were considered for the first time in [6, 7] in the simple one-dimensional analytical model by neglecting the beam divergence due to diffraction. An improved two-dimensional model was used in [8]; however, the spectral properties of the α-DFB-laser cavity were considered within the framework of the spectrally selective reflection at the laser diode facet, i.e., in the model of the spatially lumped spectral filter.

Clearly, the most comprehensive theoretical consideration of the spectral selectivity of an α-DFB laser cavity is possible only with the employment of numerical methods. In [4], a numerical model was proposed for the calculation of the spectral selectivity of the α-DFB laser cavity above the lasing threshold. In this paper the change in spectral selectivity due to the saturation effect (spatial 'hole burning') and the change in the refractive index profile caused by nonuniform self-heating of a laser diode were considered.

In the present work, the results of the experiment and corresponding numerical calculations of the spectral selectivity for the typical design of the α-DFB laser cavity are presented. Theoretical calculations were made within the framework of the Fox–Lee approach using the beam propagation method based on the fast Fourier transform [4].

In addition, the problem of determination of the intermode distance for an α-DFB laser cavity is addressed. The spectral distance between the adjacent axial modes of the conventional Fabry–Perot cavity is determined by the emission wavelength, the group refractive index and the distance between mirrors, or, in other words, by the optical path length for the emission passing through the cavity. In the case of an α-DFB laser, however, due to the winding propagation trajectory of the emission, the optical path length will not coincide with the cavity length, and its determination is a nontrivial problem requiring separate analysis. However, as it is shown below, a simple geometrical consideration yields a good agreement with the experiment.

2. Experiment

The design of an α-DFB laser under study is schematically presented in Fig. 1a. The parameters of the heterostructure layers and the phase grating parameters are given in [4, 5]. We studied samples of length 2 mm (distance between the mirrors of the laser diode), with the mirror reflection coefficients of 94 % and 1 %, the width of the active region $W = 160$ μm, the tilt angle of grating of 15° and the grating period $\Lambda = 594$ nm. The threshold current for these diodes was 840 mA and the differential efficiency was 0.48 W A^{-1}. A measured low angular divergence of emission in the lasing regime (similar to that reported in [4, 5]) confirmed the efficiency of the grating in the samples as a spatial (angular) filter.

For comparison, we also performed measurements with conventional semiconductor lasers with a Fabry–Perot cavity (without a built-in grating) with the active region width of 100 μm, the cavity length of 2 mm, and the mirror reflection coefficients of 94 % and 1 %. These lasers were manufactured of the same heterostructure as the studied α-DFB lasers and served as reference samples. The threshold current for them was 280 mA, and the differential efficiency was 0.9 W A^{-1}.

The mode gain spectra of the lasers were measured at different fixed pump currents by the modified Hakki–Paoli [9, 10] technique based on the recording of the amplified spontaneous emission (ASE) spectrum in the subthreshold regime. The mode gain value was determined from the ratio of a single longitudinal resonance width to the intermode distance. The measurements were performed at room temperature.

Figure 2 illustrates the typical examples of the measured ASE spectra for the α-DFB laser and for the Fabry–Perot cavity laser, which served as the data for finding the mode gain spectra. The general view of the measured mode gain spectrum reproduces in outline the spectral dependence of the transmission coefficient for the passive α-DFB laser cavity obtained in [7]. The intermode distance and the envelope width for the experimental curve in Fig. 2 can be, in principle, calculated within the framework of the employed model, but for the adequate description of the experiment a more realistic model is needed.

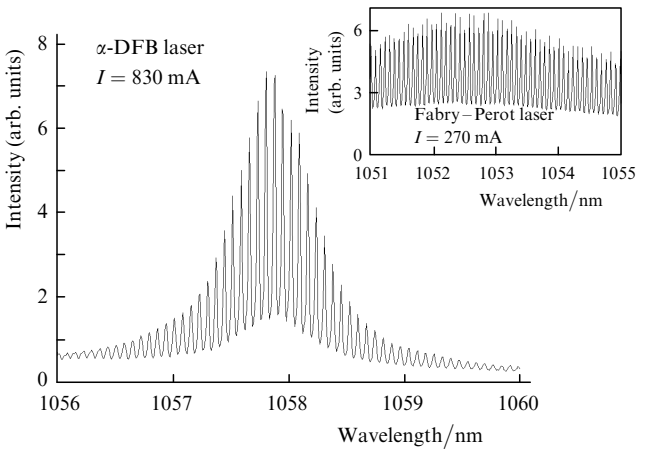

Figure 2. Amplified spontaneous emission spectrum of the α-DFB laser (in a subthreshold regime). The inset shows the similar spectrum for the Fabry–Perot laser, I is the pump current.

3. Calculation

The mode gain for the Fabry–Perot cavity laser is given by the expression:

$$g(\lambda) = \Gamma G(\lambda) - \alpha_{\mathrm{nr}}, \tag{4}$$

where Γ is the optical confinement factor which is determined from the solution of the waveguiding problem for the given heterostructure (for the samples under study, $\Gamma = 0.0132$); $G(\lambda)$ is the gain in the active region (so-called material gain); α_{nr} is the nonresonant losses in heterostructure layers (e.g., due to scattering), which depend weakly on the emission wavelength. The theoretical dependence $G(\lambda)$ was found by the method analogous to that described in [11]. The calculations were performed using an eight-band $\boldsymbol{k}\cdot\boldsymbol{p}$ Hamiltonian and taking into account all possible transitions between subbands in the quantum well. The current density was computed as a sum of the radiative part, calculated consistently with the gain, and a nonradiative part. The leakage current into the waveguide layers was calculated by assuming local charge neutrality. Although we calculated the gain in the active region by neglecting many-body effects (except for the phenomenological corrections for the gain spectral brodening with the hyperbolic secant shape and for the band-gap renormalisation), good agreement with the experiment was achieved (see Fig. 3). The value of the nonresonant losses α_{nr} used as a fitting parameter was 3 cm^{-1}.

The mode gain g for the α-DFB laser can be obtained by calculating the amplification coefficient A for the wave amplitude after the round trip in the cavity with a tilted phase grating. The coefficient A was calculated as described in [4], briefly, the procedure is as follows. Starting from some arbitrary initial field distribution at one of the cavity mirrors the series of Fox–Lee iterations are performed, going on until the field distribution does not change anymore after a successive iteration. The value of A is defined as the ratio of the field amplitude after a round trip to the field amplitude before it.

Note that for the conventional Fabry–Perot cavity laser the value of A is determined by the relation:

$$A = r_1 r_2 \exp\left[\frac{\mathrm{i}4\pi n(\lambda)L}{\lambda} + g(\lambda)L\right], \tag{5}$$

where r_1 and r_2 are the mirror reflection coefficients (with respect to the amplitude); $n(\lambda)$ is the effective (mode) refractive index; L is the cavity length. Correspondingly

$$g = \frac{1}{L}\left(\ln|A| + \ln\frac{1}{|r_1 r_2|}\right). \tag{6}$$

The spectral interval between the adjacent axial modes is related to A by the expression:

$$\delta\lambda = 2\pi\left(\frac{\partial}{\partial\lambda}\arg A\right)^{-1}, \tag{7}$$

where $\arg A$ is the argument of the complex quantity

$$A = |A|\exp(\mathrm{i}\arg A). \tag{8}$$

Expression (7) with account of (5) yields a conventional expression for the intermode interval $\delta\lambda$ in the case of the Fabry–Perot cavity laser:

$$\delta\lambda_{\mathrm{FP}} = \frac{\lambda^2}{2Ln_{\mathrm{g}}}, \quad n_{\mathrm{g}} = n - \lambda\frac{\partial n}{\partial\lambda}. \tag{9}$$

However, this expression is not applicable in the case of the α-DFB laser since it is not clear what values of L and n_{g} should be employed for the zigzag optical beam propagation between the mirrors and in the presence of possible additional mode refractive index dispersion (connected with the spectral selectivity due to the grating). Hence, the quantities g and $\delta\lambda$ for the α-DFB laser (g_α and $\delta\lambda_\alpha$) were calculated from equations (6) and (7), respectively. These relations are more general than (5) and (9), which are normally used for the Fabry–Perot cavity lasers.

4. Comparison of the experimental and calculation results

Mode gain spectra $g(\lambda)$ obtained for the Fabry–Perot cavity lasers are presented in Fig. 3. The smooth curves are calculated dependences and the noisy lines (random spread is less than 1 cm^{-1}) are experimental spectra. On the right side of the figure the values of the pump current density, at which these spectral contours have been obtained, are given.

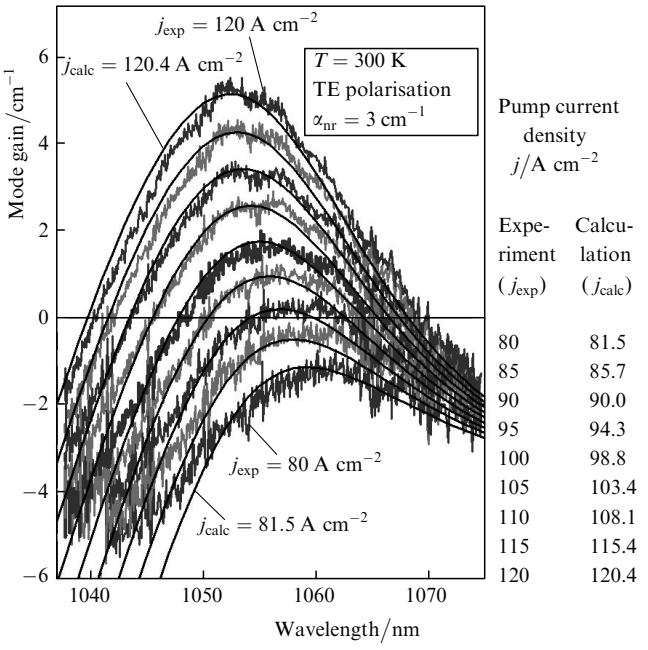

Figure 3. Calculated and experimental mode gain spectra for the studied heterostructure for different pump current densities.

Figure 4 illustrates the experimental dependence of the mode refractive index on the pump current density due to variations in the carrier concentration N in the active region. This dependence was obtained by the method described in [9, 10] taking into account the thermal contribution to the experimental dependence, caused by the self-heating of the laser diode. The derivative $\partial n/\partial T = 3.4 \times 10^{-4}$ K^{-1} was determined by independent measurements. We also determined by this method the thermal resistivity of the laser

diode (9.4 K W^{-1}), and its specific value (1.9×10^{-2}K cm^2 W^{-1}).

One can see from Fig. 4 that the dependence of Δn on j is close to linear in the subthreshold region of the investigated range of pump current densities (in our case from 75 to 140 A cm^{-2}). Thus, one can conclude that the dependence of the pump current density j on the carrier concentration N is close to linear as well. Indeed, assuming for this range of j a linear dependence $\Delta n(N)$, we can deduce from the data of Fig. 4 a relative degree of nonlinearity for the dependence $j(N)$. If one approximates the experimentally obtained dependence $j(N)$ by the expression including the linear term and the terms proportional to N^2 and N^3 (usually identified as bimolecular and Auger recombination), the contribution of the nonlinear terms will amount to less then 10 %. In other words, the rate of the carrier recombination is almost linear in N and this process can be characterised by a constant value of the carrier lifetime.

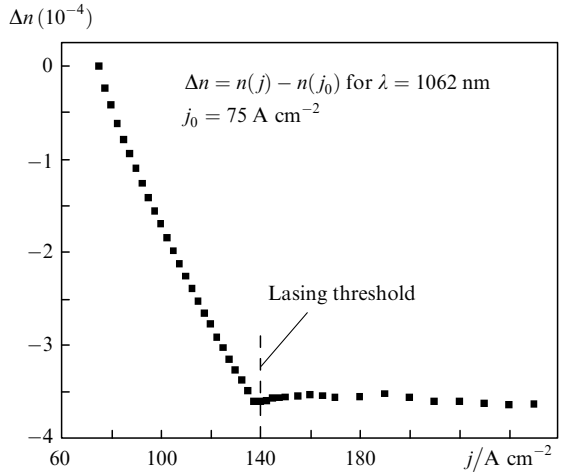

Figure 4. Change in the mode refractive index with increasing the pump current density caused by the change in the carrier concentration in the active region.

The mode gain spectra for the α-DFB laser are presented in Fig. 5. Compared to the case of the Fabry–Perot cavity laser, one can note the considerable narrowing of the spectral contours. A decrease in the width of the mode gain spectral contour is the result of the α-DFB laser cavity selectivity caused by the presence of the phase grating. However, because of the difference in the shapes of the mode gain spectral contours for the α-DFB lasers and the Fabry–Perot cavity lasers, it is more convenient to compare not their contour widths, but the contour curvatures near the maximum. As a rule, it is just the spectral region near the gain spectrum maximum that is of great interest because only within that spectral region the excitation of laser modes is possible.

The obtained spectral contours were approximated by the following expression near their maxima:

$$g(\lambda) = g(\lambda_0) - a(\lambda - \lambda_0)^2, \tag{10}$$

where $g(\lambda_0)$ is the value of the gain at the maximum; λ_0 and a are the wavelength and the contour curvature coefficient at the maximum. One can see from Fig. 5 that the value of λ_0 for the α-DFB laser is virtually independent of the pump

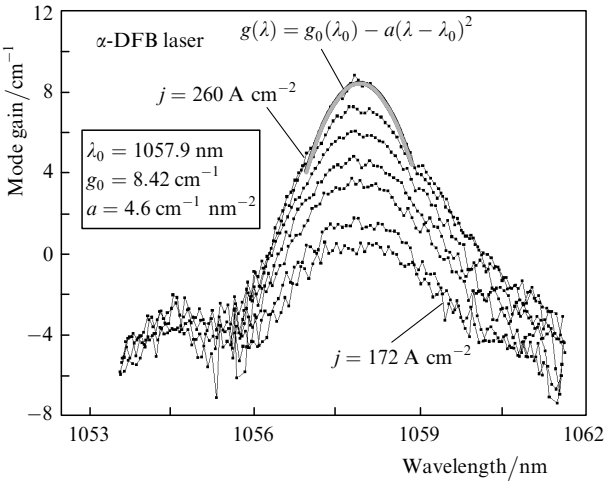

Figure 5. Experimental spectra of the mode gain g for the α-DFB laser for different pump current densities. The smooth gray curve is the parabolic approximation of one of the spectra near its maximum.

current, whereas the curvature a increases with current. For the pump current density of 260 A cm^{-2} it is equal to 4.6 cm^{-1} nm^{-2}. In the case of the Fabry–Perot cavity lasers the value of a is exclusively determined by a spectral dependence of the material gain $G(\lambda)$. For the upper curve in Fig. 3, it is equal to 3.8×10^{-2} cm^{-1} nm^{-2}. Therefore, one can state that the use of a tilted phase grating increases the effective spectral selectivity of the active medium by more than two orders of magnitude.

The effect of the narrowing of the mode gain spectral contours in the presence of the grating can be treated as their modulation by means of a narrow spectral contour $f(\lambda - \lambda_0)$, i.e. one can suppose that

$$g_\alpha(\lambda) = g(\lambda) f(\lambda - \lambda_0) \approx g(\lambda_0) f(\lambda - \lambda_0). \tag{11}$$

Then for the Lorentzian contour ($f(\Delta\lambda) \sim [1 + (\Delta\lambda/\gamma)^2]^{-1}$, where γ is the half-width of the contour at half-height), the calculated value of a for the upper curve of Fig. 5 will correspond to the half-width $\gamma = 1.45$ nm.

The results of comparison of the experimental mode gain contours of an α-DFB laser with the calculation are given in Fig. 6. The calculations were performed for the pump current density of 260 A cm^{-2} (upper experimental curve in Fig. 5). The calculations were made for two cases. In the first case it was supposed that the value of the phase grating amplitude δn in (1) is independent of the wavelength, i.e., $\partial(\delta n)/\partial\lambda \equiv 0$. The obtained curve (shown by a dotted line in Fig. 6) differs noticeably from the experimental one. In the second case, the calculations were performed with the assumption of a possible spectral dispersion of δn. Assuming $\partial(\delta n)/\partial\lambda = -0.15$ μm^{-1} a good agreement with the experiment was achieved (a solid curve in Fig. 6). Our attempts to improve the agreement between the calculated and experimental curves at the expense of introducing the dispersion for other cavity parameters have failed. From Fig. 6 one can conclude that the dispersion of the phase grating amplitude δn may play an important role in the formation of the spectral selectivity of the α-DFB laser cavity. Although the fitting value for the dispersion of δn does not seem strange, we are not yet able to explain what physical mechanism might be responsible for it.

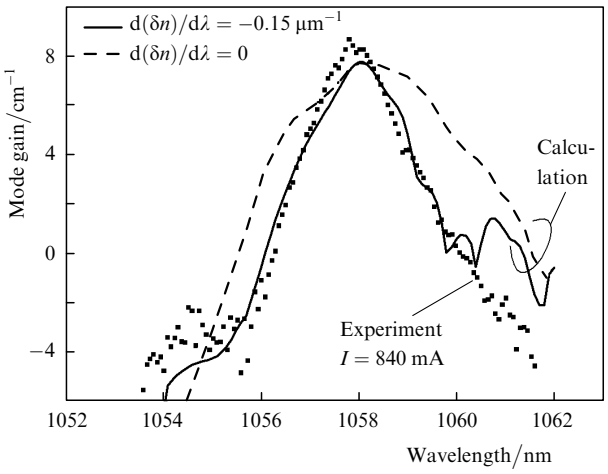

Figure 6. Comparison of the experimental mode gain spectrum of the α-DFB laser (dots) with the calculated one taking into account (solid curve) and neglecting (dashed curve) the dispersion of the phase grating amplitude $d(\delta n)/d\lambda$.

A more detailed analysis of the experimental mode gain spectra (Fig. 6) reveals a certain random scatter of points near the curve maximum. This randomness may not be attributed to the measurement accuracy since the observed experimental spread of data was larger than the measurement error. The most probable reason for such a scatter is the presence of spatial optical inhomogeneities inside the cavity. The influence of such inhomogeneities on the spectral properties of laser was described earlier (see, for example, [12–14]).

The phase grating in the cavity changes the effective optical path of the emission passing from one mirror to another, and so the intermode distance $\delta\lambda$. The value of $\delta\lambda_\alpha$ found from the ASE spectrum (see Fig. 2) near $\lambda = 1058$ nm is 7.2×10^{-2} nm. The value of $\delta\lambda_\alpha$ calculated in accordance with (7) for the corresponding laser cavity parameters was 7.23×10^{-2} nm, which agrees well with the experimental result. The obtained value of $\delta\lambda_\alpha$ allows one to determine the effective optical path length for the emission propagating inside the α-DFB laser cavity. According to equation (9) we obtain:

$$(n_g L)^{\text{eff}} = \frac{\lambda^2}{2\delta\lambda_\alpha}. \tag{12}$$

In our case, this quantity is 7.77 mm. Note that in the case of an α-DFB laser only the product $(n_g L)^{\text{eff}}$ can be determined, neither n_g^{eff} nor L^{eff} can be found separately. As for the Fabry–Perot cavity lasers, the quantity L in equation (9) is just the length of the cavity, so once the value of the intermode distance is known, the group refractive index can be easily found. In our experiment we obtained $\delta\lambda_{\text{FP}} = 7.7 \times 10^{-2}$ nm (near $\lambda = 1058$ nm), which yields $n_g = 3.634$.

The observed decrease in the intermode distance in the case of an α-DFB laser as compared to a Fabry–Perot cavity laser (with the same cavity length), from $\delta\lambda_{\text{FP}} = 7.7 \times 10^{-2}$ nm to $\delta\lambda_\alpha = 7.2 \times 10^{-2}$ nm, can be explained to a good accuracy in the following way. As it has been already stated, the emission propagates inside the α-DFB laser cavity in zigzag (see Fig. 1b), and the geometrical length of such a trajectory from one mirror to another is equal to

$$L^{\text{eff}} = \frac{L}{\cos^2\alpha}. \tag{13}$$

Because the α-DFB lasers were made of the same heterostructure as the Fabry–Perot lasers, we can set $n_g^{\text{eff}} = n_g = 3.634$ (we neglect the difference in refractive indices caused by the difference in pump levels). For $L = 2$ mm, we obtain from (12) and (13) $(n_g L)^{\text{eff}} = 7.79$ mm, $\delta\lambda_\alpha = 7.18 \times 10^{-2}$ nm, which is close to the experimental values.

5. Conclusions

We have shown experimentally and by numerical calculations that the active medium of the α-DFB laser not only performs the spatial filtering of the optical beam but also also possess a spectral selectivity, which limits the spectral contour width of the effective mode gain. The half-width at half-maximum of such a contour was 1.45 nm for the studied lasers, in the Lorentzian approximation for the gain spectrum near its maximum. The high selectivity of the α-DFB laser cavity facilitates an establishment of the single-mode (single-frequency) lasing in the wide range of pump currents.

The calculation has shown that the width of the spectral contour of an α-DFB laser gain may be influenced by the dispersion of the phase grating amplitude.

The experimentally measured value of the intermode distance for the α-DFB laser is in a good agreement with the value, calculated within the framework of a numerical model. The decrease in the intermode distance as compared to the case of a Fabry–Perot laser can be regarded as a consequence of the increasing of the effective optical path length by the geometrical factor $\cos^{-2}\alpha$, which is connected with the zigzag propagation of emission inside the cavity.

The experimental results indicate that the dependence of the pump current density on the carrier concentration is close to linear in the studied region (from 75 to 140 A cm^{-2}) and can be characterised by a constant carrier lifetime.

References

1. Dzurko K.M., Lang R.J., Welch D.F., Scofres D.R., Hardy A. *Proc. IEEE/LEOS Ann. Meet.* (San Fransisco, CA, 1995) Vol. 2, p. 400.
2. Wong V.V., DeMars S.D., Schönfelder A., Lang R.J. *Proc. CLEO* (San Francisco, CA, 1998) p. 34.
3. Popovichev V.V., Davydova E.I., Marmalyuk A.A., Simakov A.V., Uspenskii M.B., Chel'nyi A.A., Bogatov A.P., Drakin A.E., Plisyuk S.A., Stratonnikov A.A. *Kvantovaya Elektron.*, **32** (12), 1099 (2002) [*Quantum Electron.*, **32** (12), 1099 (2002)].
4. Paschke K., Bogatov A., Drakin A., Güther R., Stratonnikov A.A., Wenzel H., Erbert G., Trankle G. *IEEE J. Sel. Top. Quantum Electron.*, **9** (3), 835 (2003).
5. Paschke K., Bogatov A., Bugge F., Drakin A., Fricke J. Güther R., Stratonnikov A., Wenzel H., Erbert G., Trankle G. *IEEE J. Sel. Top. Quantum Electron.*, **9** (5), 1172 (2003).
6. Güther R. *Proc. SPIE Int. Soc. Opt. Eng.*, **3737**, 448 (1999).
7. Güther R. *J. Opt. A: Pure Appl. Opt.*, **1**, 417 (1999).
8. Sarangan A.M., Wright M.W., Marciante J.R., Bossert D.J. *IEEE J. Quantum Electron.*, **35** (8), 1220 (1999).
9. Bogatov A.P., Boltaseva A.E., Drakin A.E., Belkin M.A., Konyaev V.P. *Kvantovaya Elektron.*, **30** (4), 315 (2000) [*Quantum Electron.*, **30** (4), 315 (2000)].
10. Bogatov A.P., Boltaseva A.E., Drakin A.E., Belkin M.A., Konyaev V.P. *Fiz. Tekh. Poluprovod.*, **34** (10), 1207 (2000).

11. Wenzel H., Erbert G., Enders P.M. *IEEE J. Sel. Top. Quantum Electron.*, **5** (3), 637 (1999).
12. Bezotosnyi V.V., Bogatov A.P., Dolginov L.M., Drakin A.E., Eliseev P.G., Mil'vidskii M.G., Sverdlov B.N., Shevchenko E.G. *Trudy FIAN*, **141**, 18 (1983).
13. Klehr A., Beister G., Erbert G., Klein A., Maege J., Rechenberg I., Sebastian J., Wenzel H., Trankle G. *J. Appl. Phys.*, **90** (1), 43 (2001).
14. Lewis G.M., Smowton P.M., Thomson J.D., Summers H.D., Blood P. *Appl. Phys. Lett.*, **80** (1), 1 (2002).